

A neurodynamic optimization approach to TDOA-based IoT localization in NLOS environments

Wenxin Xiong^{a,*}, Christian Schindelhauer^a, Hing Cheung So^b, Junli Liang^c,
Zhi Wang^d

^a*Department of Computer Science, University of Freiburg, Freiburg 79110, Germany*

^b*Department of Electrical Engineering, City University of Hong Kong, Hong Kong, China*

^c*School of Electronics and Information, Northwestern Polytechnical University, Xi'an 710072, China*

^d*State Key Laboratory of Industrial Control Technology, Zhejiang University, Hangzhou 311121, China*

Abstract

Time-difference-of-arrival (TDOA) localization using unreliable data collected by the Internet of Things (IoT) sensors in non-line-of-sight (NLOS) environments is considered herein. We exploit a hardware realizable neurodynamic optimization model, with the use of a Welch M -estimator based loss function to enhance the robustness to outliers. Since the outlying nature of NLOS bias is covered when generating the TDOAs from IoT-sensor-gathered timestamps, we propose to retrieve the underlying time-of-arrival components during the problem formulation by jointly estimating the source position and onset time. A projection-type neural network (PNN) based on the redefined augmented Lagrangian and projection theorem is then applied to solve the derived non-convex constrained optimization problem, whose local stability of equilibrium is examined and discrete implementation complexity is analyzed. Simulation investigations show that our neurodynamic TDOA localization solution is superior to several existing schemes in terms of localization accuracy, especially when the NLOS paths and errors tend to exhibit sparsity and severeness, respectively.

Keywords: Non-line-of-sight, time-difference-of-arrival localization, Internet of Things, Welch M -estimator, neurodynamic optimization

*Corresponding author

Email address: xiongw@informatik.uni-freiburg.de (Wenxin Xiong)

1. Introduction

Internet of Things (IoT) intending to provide end-to-end connectivity among sensors and actuators requires fine-grained location information for organizing the huge amounts of data from heterogeneous devices [1]. In the more general cases where Global Positioning System services or manual deployment may not be available, source localization using some form of signal measurements (e.g., time-of-arrival (TOA) and time-difference-of-arrival (TDOA)) from coordinated IoT sensors is often counted on to fulfill the task [2].

TDOA defined as the difference in the signal arrival timestamps collected at a pair of sensors removes the need for clock synchronization between the source and sensors [3, 4, 40, 6], and therefore has been a fine option in the IoT context [7, 8]. These algorithms, devised under the Gaussian assumption of noise, however, might fail to work properly when outlying data exist. As a primary source of outliers, non-line-of-sight (NLOS) propagation often takes place when there are obstructions in the direct transmission path, and has in fact been widely reported in the positioning literature [9, 10, 11, 12, 13, 14, 15, 16, 20, 21, 17, 18, 19, 22, 23]. With respect to (w.r.t.) TDOA-based localization, the pursuit of outlier-resistance becomes somewhat more complicated than the well-studied TOA counterpart, because of the potential reductions during the computation of TDOAs from the sensor-collected timestamps [17]. Thus, simply modeling the possible NLOS error in a TDOA measurement as an outlying value (e.g. [12, 13, 14]) may be even unrealistic. This raises some degree of difficulty in the problem formulation, and commonly-used countermeasures include the identifying and discarding (IAD) process [15, 16], worst-case (WC) criterion [17, 19, 18], and model transformation [20, 21] (details can be found in Section 2). In this paper, we follow the third path and aim to rebuild the underlying TOA components in which the non-Gaussian noise preserves the impulsive feature.

Unlike traditional numerical schemes that are realized and run on digital computers, neurodynamic optimization based on analog neuromorphic circuits

admits real-time and parallel physical implementations [25, 26, 24, 27, 28, 29], and fits in perfectly with the IoT smart sensors where efficient computing is required [30]. Following the pioneering work of Hopfield and Tank [24], substantial progress has been made in recurrent neural networks (NNs) [25, 26, 27, 28, 29], with the projection-type NN (PNN) based on the projection theorem and a re-defined augmented Lagrangian being an emerging framework for solving general constrained optimization problems (GCOPs) [25]. Nevertheless, PNN finds only scant application in localization [21].

The main contribution of this work is to devise an outlier-robust and hardware implementable neurodynamic TDOA localization technique for the IoT infrastructure deployed in NLOS environments. It is worth pointing out that invoking our proposed method requires merely the sensor positions, reception timestamps collected by the sensors, and signal propagation speed as prior information. Based on the joint estimation of the source position and time at which the source emits the signal, a robust loss function associated with the Welsch M -estimator: $1 - \kappa_\sigma(\cdot) = 1 - (\exp(-(\cdot)^2/2\sigma^2))$ is used for improving the resilience of IoT system (see 1 for an illustration). The Welsch M -estimator has been successfully utilized in numerous areas of science and engineering [32, 33, 34, 35], but rarely seen in the context of TDOA-based passive source localization. Despite the foundation resemblance laid in the Lagrange multiplier theory between our neurodynamic approach and those [31, 21], it should be noted that we rely on the error function of the Welsch M -estimator, thus giving rise to a problem formulation distinct from the counterparts of ℓ_2 loss $(\cdot)^2/2$ in [31] and ℓ_1 loss $|\cdot|$ in [21]. Being undoubtedly more robust than the conventional ℓ_2 criterion, the Welsch loss also has the benefit that it is statistically more efficient compared to the ℓ_1 loss [33].

The remainder of the paper is organized as follows. Sections 2 and 3 briefly review the state-of-the-art TDOA localization schemes and formulate the problem to be solved, respectively. In Section 4, the neurodynamic optimization framework is established, whose convergence property and discrete implementation complexity are also discussed. For the evaluation of performance, numerical

results are included in Section 5. Finally, conclusions are drawn in Section 6.

2. Related work

The authors of [15] and [16] map out separate IAD strategies to reject the outlier-prone TDOA measurements. In spite of their simplicity, we note that false-alarms and missed-detections are generally inescapable in the implementation of the threshold-dependent IAD schemes. In [20], the authors put forward the idea of TDOA-to-TOA model transformation, in a sense that the dropped source onset time can be re-added by treating it as a confined optimization variable. Just like the original study on TOA-based systems in [22] from which [20] is derived, semidefinite programming (SDP) is taken advantage of to cope with a nonlinear least squares (LS) problem built upon small Gaussian disturbance assumption. Benefiting from the strong resistance to outliers, WC-based tactics have lately attracted considerable attention among researchers [17, 19, 18]. Concretely, the WC criterion is leveraged to robustify the estimator, and convex relaxation is then employed to handle those intricate optimization problems. With the use of the second-order cone programming or SDP solvers, the methods in [20, 17, 19, 18], however, may not be preferred in the real-world IoT applications as they are computationally costly. Furthermore, additional prior information of error bounds is needed provided the WC criterion is to be invoked.

Another appealing way of estimator robustification is to trim the loss function in fitting errors [36], as not explicitly introducing parameters for the noise-related terms may lead to more cost-effective approaches. In particular, since large errors can dominate the ℓ_2 measure (e.g. [31]) which is optimal only under Gaussianity, NN is put into use in [21] for solving the robustified TDOA formulation based on ℓ_1 -minimization and model transformation. Equipped with a neurodynamic framework, such a method, as well as the ℓ_2 loss counterpart in [31], have the merits of being physically realizable and delivering real-time solutions with theoretically guaranteed optimality [29, 25, 26, 24, 27, 28].

3. Problem formulation

Our localization scenario consists of $L \geq k+1$ coordinated IoT smart sensors and a single source to be located in k -dimensional space ($k = 2$ or 3). The known position of the i th sensor and unknown source location are denoted by $\mathbf{x}_i \in \mathbb{R}^k$ (for $i = 1, 2, \dots, L$) and $\mathbf{x} \in \mathbb{R}^k$, respectively. In a passive manner, a radio or sound signal is emitted from the source at an unknown onset time t_0 , and received by the i th sensor (for $i = 1, 2, \dots, L$) at time t_i afterwards, where t_i corresponds to the available received signal timestamp thereat. The TOA measurement between the i th sensor and source can be modeled as

$$t_i - t_0 = \frac{1}{c} (\|\mathbf{x} - \mathbf{x}_i\|_2 + n_i + q_i), \quad i = 1, 2, \dots, L, \quad (1)$$

where c is the signal propagation speed, $\|\cdot\|_2$ represents the ℓ_2 -norm of a vector, n_i is assumed to be zero-mean Gaussian noise with variance σ_i^2 , $q_i = \begin{cases} e_i, & \text{if the } i\text{th source-sensor path is NLOS} \\ 0, & \text{if the } i\text{th source-sensor path is LOS} \end{cases}$, and e_i is a positive bias. However, (1) is unavailable in our considered setting where the source onset time is unknown due to the lack of clock synchronization between the source and any sensor. By designating the first sensor as the reference, the nonredundant TDOAs are calculated instead as

$$t_{i,1} = \frac{1}{c} (\|\mathbf{x} - \mathbf{x}_i\|_2 - \|\mathbf{x} - \mathbf{x}_1\|_2 + n_{i,1} + b_{i,1}) = t_i - t_1, \quad i = 2, 3, \dots, L, \quad (2)$$

where $n_{i,1} = n_i - n_1$ and $b_{i,1} = q_i - q_1$ (both for $i = 2, 3, \dots, L$) are the cumulative noise and NLOS error in the corresponding range-difference (RD) measurement.

Similar to [20] and [21], t_0 is taken as an additional estimation variable for bypassing the intractability that $e_{i,1}$ is not necessarily an outlier. In doing so we aim at solving

$$\min_{t_0, \mathbf{x}} \sum_{i=1}^L f_r((t_i - t_0)c - \|\mathbf{x} - \mathbf{x}_i\|_2), \quad (3)$$

where $f_r(\cdot)$ is some robust loss function exhibiting resistance to the NLOS bias. This strategy is also known as (a.k.a.) model transformation in the literature

[20, 21], in a sense that outlier-robustness is pursued w.r.t. $n_i + q_i$ in the TOA components instead of the TDOA counterpart $n_{i,1} + b_{i,1}$ via (3). Here, we do not introduce any additional optimization variables w.r.t. n_i or q_i .

In our case, $f_r(\cdot) = 1 - \kappa_\sigma(\cdot)$ with parameter σ is formed by drawing on the loss function of the Welsch M -estimator (see Section 1 for the definition). The Welsch M -estimator possesses a score function with strongly redescending property, making it more robust to outliers compared to the traditional Huber and Cauchy M -estimators [34, 33]. On the other hand, it is not as threshold-dependent as the Tukey M -estimator, though the latter is capable of completely rejecting the large residuals [36]. In fact, our considered Welsch loss has a very close relationship with the correntropy in information theoretic learning (ITL) [35], which is a generalized, local, and nonlinear similarity measure between two arbitrary random variables and has lately seen tremendous growth in nonlinear and non-Gaussian signal processing [37]. From this perspective, the Welsch loss likewise enjoys smooth controllability of all of its properties by σ (a.k.a. the kernel size in ITL). We provide in Fig. 1 a comparison among $1 - \kappa_\sigma(z)$, $|z|$, and $\text{Huber}(z) = \begin{cases} (1/2)z^2, & |z| \leq 1 \\ |z| - 1/2, & |z| > 1 \end{cases}$ for illustrative purpose. Apparently, the outliers can be effectively mitigated via the nonconvex Welsch loss by selecting a proper σ while on the other hand, without unduly influencing the measure when the error is close to zero.

Next, we proceed with the formulation derivation on the basis of (3). To avoid ill-posing in the subsequent gradient computation w.r.t. \mathbf{x} , auxiliary variables $\mathbf{d} = [d_1, d_2, \dots, d_L]^T \in \mathbb{R}^L$ are introduced for moving the terms of $\|\mathbf{x} - \mathbf{x}_i\|_2$ into the constraints, and therewith expressing the source-sensor distance constraints in a quadratic form [31]. As a result, we have the following substitute

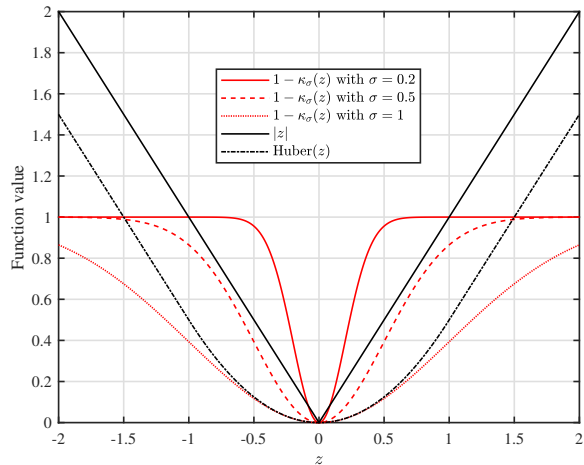


Fig. 1. Comparison of different loss functions.

for (3):

$$\min_{t_0, \mathbf{x}} - \sum_{i=1}^L \exp \left\{ - \frac{[(t_i - t_0)c - \|\mathbf{x} - \mathbf{x}_i\|_2]^2}{2\sigma^2} \right\}$$

$$\text{s.t. } 0 \leq t_0 \leq t_i, \quad i = 1, 2, \dots, L, \quad (4a)$$

$$(t_i - t_0)c + (t_j - t_0)c \geq \|\mathbf{x}_i - \mathbf{x}_j\|_2, \quad i \neq j, \quad i, j = 1, 2, \dots, L, \quad (4b)$$

$$(t_i - t_0)c \geq d_i, \quad i = 1, 2, \dots, L, \quad (4c)$$

where (4a), (4b), and (4c) are the temporal constraints for binding the nuisance variable t_0 , geometrical constraints by the triangle inequality, and constraints based on the general consensus that e_i is much greater than $|n_i|$, respectively [20, 21]. It is noteworthy that (4b) and (4c) may not be satisfied in certain cases where n_i is negative and q_i is of small magnitude. This will result in an infeasible program if convex programming is applied [23, 20]. In what follows, we design a PNN for coping with (4), which offers somewhat softening and will not be encumbered by the infeasibility issues.

4. PNN design

In this section, we turn our attention to the development of a PNN scheme for dealing with (4).

4.1. Framework of PNN

Let us start with considering the following paradigm of the GCOP without convexity assumptions:

$$\min_{\mathbf{z} \in \mathbb{R}^N} f(\mathbf{z}), \quad \text{s.t. } \mathbf{g}(\mathbf{z}) \leq \mathbf{0}_K, \quad \mathbf{h}(\mathbf{z}) = \mathbf{0}_M, \quad (5)$$

where $f : \mathbb{R}^N \rightarrow \mathbb{R}$, $\mathbf{g}(\mathbf{z}) = [g_1(\mathbf{z}), g_2(\mathbf{z}), \dots, g_K(\mathbf{z})]^T \in \mathbb{R}^K$ and $\mathbf{h}(\mathbf{z}) = [h_1(\mathbf{z}), h_2(\mathbf{z}), \dots, h_M(\mathbf{z})]^T \in \mathbb{R}^M$ are the K - and M -dimensional vector-valued functions (both of N variables), $f(\mathbf{z})$ and $h_i(\mathbf{z})$ (for $i = 1, 2, \dots, M$) are assumed to be all twice differentiable, $\mathbf{0}_K \in \mathbb{R}^K$ and $\mathbf{0}_M \in \mathbb{R}^M$ denote the $K \times 1$ and $M \times 1$ all-zero vectors, respectively, $\mathbf{a} \leq \mathbf{b}$ is the vector inequality which means $[\mathbf{a}]_i \leq [\mathbf{b}]_i$ ($\forall i$), and $[\cdot]_i$ denotes the i th element of a vector.

In cases when $f(\mathbf{z})$ or $g_i(\mathbf{z})$ (for $i = 1, 2, \dots, K$) is nonconvex, or $h_i(\mathbf{z})$ (for $i = 1, 2, \dots, M$) is not an affine expression, (5) does not constitute a disciplined convex programming problem, and finding the global minimizer (namely, global optimization) can be far more difficult. Comparatively speaking, it would be easier to resort to some locally stable neurodynamic optimization method [21, 31, 25, 26, 28, 24, 27], whose equilibrium state is reached at a Karush-Kuhn-Tucker (KKT) point (viz., a point satisfying the first-order necessary conditions of optimality) of (5). In order to directly take the inequality constraints into account and avoid introducing slack variables, we turn to a PNN solution derived based on the projection theorem and a re-defined augmented Lagrangian of (5): $\mathcal{L}_\rho(\mathbf{z}, \boldsymbol{\nu}) = f(\mathbf{z}) + \boldsymbol{\mu}^T \mathbf{g}(\mathbf{z}) + \boldsymbol{\lambda}^T \mathbf{h}(\mathbf{z}) + \frac{\rho}{2} \left\{ \sum_{i=1}^K [\mu_i g_i(\mathbf{z})]^2 + \sum_{i=1}^M [\lambda_i h_i(\mathbf{z})]^2 \right\}$, where $\boldsymbol{\nu} = [\boldsymbol{\mu}^T, \boldsymbol{\lambda}^T]^T \in \mathbb{R}^{K+M}$, $\boldsymbol{\mu} = [\mu_1, \mu_2, \dots, \mu_K]^T \in \mathbb{R}^K$ and $\boldsymbol{\lambda} = [\lambda_1, \lambda_2, \dots, \lambda_M]^T \in \mathbb{R}^M$ are vectors containing Lagrange multipliers for the inequality constraints and equality constraints in (5), respectively, and $\rho > 0$ is the augmented Lagrangian parameter. Descriptions of the time-domain transient behavior of PNN for addressing (5) are given

as

$$\begin{aligned}\frac{d\mathbf{z}}{dt} &= -\nabla_{\mathbf{z}}\mathcal{L}_{\rho}(\mathbf{z}, \boldsymbol{\nu}), \\ \frac{d\mu_i}{dt} &= -\mu_i + [\mu_i + g_i(\mathbf{z})]^+, i = 1, \dots, K, \quad \frac{d\boldsymbol{\lambda}}{dt} = \mathbf{h}(\mathbf{z}),\end{aligned}\quad (6)$$

where the operator $\nabla_{\mathbf{z}}(\cdot) \in \mathbb{R}^N$ denotes the gradient of some function at \mathbf{z} , and $[\cdot]^+ = \max(\cdot, 0)$ in fact defines a nonlinear projection acting like the unit ramp function. Being a recurrent neural network, the PNN assigns physical meanings to \mathbf{z} and $\boldsymbol{\nu}$ that they record the activities of the so-called *variable neurons* and *Lagrangian neurons*, respectively. The former are responsible for finding a minimum point of the objective function $f(\mathbf{z})$, while the latter take charge of guiding the dynamic trajectory into the feasible region.

Back to our robust TDOA-based localization problem, (4) clearly coincides with the GCOP (5) as long as we have the following redefinition: $N = L + k + 1$, $K = \frac{L^2+5L+2}{2}$, $M = L$, $\mathbf{z} = [t_0, \mathbf{x}^T, \mathbf{d}^T]^T \in \mathbb{R}^{L+k+1}$, $f(\mathbf{z}) = -\sum_{i=1}^L \exp\left\{-\frac{[(t_i-t_0)c-d_i]^2}{2\sigma^2}\right\}$, $g_1(\mathbf{z}) = -t_0$, $g_{i+1}(\mathbf{z}) = t_0 - t_i$ (for $i = 1, 2, \dots, L$), $g_{i+L+1}(\mathbf{z}) = -d_i$ (for $i = 1, 2, \dots, L$), $g_{i+2L+1}(\mathbf{z}) = d_i - (t_i - t_0)c$ (for $i = 1, 2, \dots, L$), $g_{\frac{(2L-i)(i-1)}{2}+j-i+3L+1}(\mathbf{z}) = g_{i,j}(\mathbf{z}) = (2t_0 - t_i - t_j)c + \|\mathbf{x}_i - \mathbf{x}_j\|_2$ (for $i = 1, 2, \dots, L-1$, $j = i+1, i+2, \dots, L$), and $h_i(\mathbf{z}) = d_i^2 - \|\mathbf{x} - \mathbf{x}_i\|_2^2$ (for $i = 1, 2, \dots, L$). For ease of exposition, the single NN presented in this paper is succinctly termed Welsch-PNN. Just as its name implies, Welsch-PNN leverages a Welsch M -estimator based loss function to reduce the adverse effects of NLOS bias and, in particular, a locally stable PNN is applied to find a strict local minimum of the related nonconvex COP. The gradient calculations in (6) are detailed as follows.

$$\frac{d\mathbf{z}}{dt} = -\left[\frac{\partial\mathcal{L}_{\rho}(\mathbf{z}, \boldsymbol{\nu})}{\partial t_0}, \left(\frac{\partial\mathcal{L}_{\rho}(\mathbf{z}, \boldsymbol{\nu})}{\partial \mathbf{x}}\right)^T, \left(\frac{\partial\mathcal{L}_{\rho}(\mathbf{z}, \boldsymbol{\nu})}{\partial \mathbf{d}}\right)^T\right]^T$$

$$\frac{\partial\mathcal{L}_{\rho}(\mathbf{z}, \boldsymbol{\nu})}{\partial \mathbf{d}} = \left[\frac{\partial\mathcal{L}_{\rho}(\mathbf{z}, \boldsymbol{\nu})}{\partial d_1}, \dots, \frac{\partial\mathcal{L}_{\rho}(\mathbf{z}, \boldsymbol{\nu})}{\partial d_L}\right]^T$$

$$\begin{aligned}
\frac{\partial \mathcal{L}_\rho(\mathbf{z}, \boldsymbol{\nu})}{\partial t_0} &= \sum_{i=1}^L \frac{c[d_i - (t_i - t_0)c]}{\sigma^2} \exp \left\{ -\frac{[(t_i - t_0)c - d_i]^2}{2\sigma^2} \right\} - \mu_1 + \sum_{i=1}^L \mu_{i+1} \\
&+ c \sum_{i=1}^L \mu_{i+2L+1} + 2c \sum_{i=1}^{L-1} \sum_{j=i+1}^L \mu_{\frac{(2L-i)(i-1)}{2} + j - i + 3L + 1} \\
&+ \rho \left\{ \mu_1^2 t_0 + \sum_{i=1}^L \mu_{i+1}^2 (t_0 - t_i) + c \sum_{i=1}^L \mu_{i+2L+1}^2 [d_i - (t_i - t_0)c] \right. \\
&\left. + 2c \sum_{i=1}^{L-1} \sum_{j=i+1}^L \mu_{\frac{(2L-i)(i-1)}{2} + j - i + 3L + 1}^2 [(2t_0 - t_i - t_j)c + \|\mathbf{x}_i - \mathbf{x}_j\|_2] \right\}
\end{aligned}$$

$$\frac{\partial \mathcal{L}_\rho(\mathbf{z}, \boldsymbol{\nu})}{\partial \mathbf{x}} = 2 \sum_{i=1}^L (\mathbf{x} - \mathbf{x}_i) \left[\rho \lambda_i^2 (\|\mathbf{x} - \mathbf{x}_i\|_2^2 - d_i^2) - \lambda_i \right]$$

$$\begin{aligned}
\frac{\partial \mathcal{L}_\rho(\mathbf{z}, \boldsymbol{\nu})}{\partial d_i} &= \frac{[d_i - (t_i - t_0)c]}{\sigma^2} \exp \left\{ -\frac{[(t_i - t_0)c - d_i]^2}{2\sigma^2} \right\} - \mu_{i+L+1} + \mu_{i+2L+1} \\
&+ 2\lambda_i d_i + \rho \left\{ \mu_{i+L+1}^2 d_i + \mu_{i+2L+1}^2 [d_i - (t_i - t_0)c] + 2\lambda_i^2 d_i (d_i^2 - \|\mathbf{x} - \mathbf{x}_i\|_2^2) \right\}, \\
&i = 1, 2, \dots, L.
\end{aligned}$$

4.2. Local stability

According to the previous research in [25, 21, 26], PNN governed by (6) is assured locally stable, in other words will reach equilibrium at a KKT point $(\mathbf{z}^*, \boldsymbol{\nu}^*)$ for (5) under very mild conditions, where \mathbf{z}^* is a strict local minimum of (5). With a large enough ρ , the sufficient conditions for its local stability can be summarized as: (i) the gradients of the equality constraints and active inequality constraints w.r.t. \mathbf{z} are linearly independent at the feasible point; and (ii) the Hessian of the restricted Lagrangian at a KKT point is positive definite on the critical cone. Since there would be no need for localization in scenarios with $d_i = 0$ (namely, the positions of the i th sensor and source coincide), none of our inequality constraints are active. We may only calculate the gradient of

$\mathbf{h}(\mathbf{z})$ w.r.t. \mathbf{z} at a KKT point¹ $(\mathbf{z}^*, \boldsymbol{\nu}^*)$ for verifying (i), i.e.

$$\nabla_{\mathbf{z}} \mathbf{h}(\mathbf{z}^*) = \left[\mathbf{0}_L \mid 2 \left(\mathbf{X}^T - \mathbf{1}_L \mathbf{x}^{*T} \right) \mid 2 \text{diag}(\mathbf{d}^*) \right], \quad (8)$$

where $\mathbf{X} = [\mathbf{x}_1, \dots, \mathbf{x}_L] \in \mathbb{R}^{k \times L}$, $\mathbf{1}_L \in \mathbb{R}^L$ denotes an all-one vector of length L , and $\text{diag}(\cdot)$ is a diagonal matrix with the corresponding vector as main diagonal. We see that the row vectors of the matrix in (8) are linearly independent, again on the premise of $d_i^* \neq 0$ (for $i = 1, 2, \dots, L$). Combining the inactivity of inequality constraints and linear independence just verified further deduces an empty critical cone [25, 21, 26]. Consequently, the two conditions are both met and the local stability of Welsch-PNN is confirmed.

4.3. Remarks on algorithm implementation

In terms of the number of neurons, the PNN herein involves $(L^2 + 9L)/2 + k + 2$ neurons in total, indicating in some sense its circuit complexity. As an analog neural computational technique aiming to deliver real-time solution in the IoT context, it is not meaningful to compare the PNN's circuit complexity with the algorithmic complexities of the existing digital methods (e.g. [20, 17, 18, 19]). Nonetheless, PNN can still be realized in a numerical and discrete fashion [38], if it has to be. We summarize in (9) the steps of iteratively and numerically realizing Welsch-PNN:

$$\mathbf{z}_{(\kappa+1)} = \mathbf{z}_{(\kappa)} + \tau \frac{d\mathbf{z}}{dt}, \quad \boldsymbol{\mu}_{(\kappa+1)} = \boldsymbol{\mu}_{(\kappa)} + \tau \frac{d\boldsymbol{\mu}}{dt}, \quad \boldsymbol{\lambda}_{(\kappa+1)} = \boldsymbol{\lambda}_{(\kappa)} + \tau \frac{d\boldsymbol{\lambda}}{dt}, \quad (9)$$

where the dynamics of the derivatives $\frac{d\mathbf{z}}{dt}$ and $\frac{d\boldsymbol{\lambda}}{dt}$ have been predefined and $\tau > 0$ is the step size. Note that the iteration index is indicated through the use of the subscript $(\cdot)_{(\kappa)}$. The procedure in (9) also enables us to in a way quantify the computational overheads of Welsch-PNN. The quantification is based on the assumption that the update of values held in neurons dominates the computational cost of each iteration, and the fact that evaluation operation of a

¹For notational convenience, we assume that the asterisk in the superscript of a vector applies to each element of that vector by default.

Table 1: Summary of considered NLOS mitigation algorithms

Algorithm	Input	Complexity
Welsch-PNN	Sensor positions Received signal timestamps Signal propagation speed	$\mathcal{O}(N_{\text{PNN}}L^2)$
SDP-Robust-Refinement-1	Sensor positions TDOA-based RD measurements Upper bounds on NLOS errors	$\mathcal{O}(L^{6.5})$
SDP-Robust-Refinement-2	Sensor positions TDOA-based RD measurements Upper bounds on NLOS errors	$\mathcal{O}(L^{6.5})$
SDP-TOA	Sensor positions Received signal timestamps Signal propagation speed	$\mathcal{O}(L^4)$

degree- n polynomial with fixed-size coefficients using Horner’s method [39] has a complexity of $\mathcal{O}(n)$. As a consequence, the discrete realization complexity of Welsch-PNN is $\mathcal{O}(N_{\text{PNN}}L^2)$, where N_{PNN} denotes the number of iterations taken in discretely realizing the PNN. Table 1 gives an overview of different NLOS-resistant TDOA-based localization techniques considered for comparison, including our Welsch-PNN scheme, SDP-based robust method for solving Formulation 1 in [18] (termed SDP-Robust-Refinement-1), SDP-based robust method for solving Formulation 2 in [18] (termed SDP-Robust-Refinement-2), and SDP-based model transformation method in [20] (termed SDP-TOA).

5. Numerical results

In this section, computer simulations are carried out to substantiate the efficacy of Welsch-PNN in comparison with other schemes showcased in Table 1. A popularly used non-robust TDOA-based localization scheme in [40], named separated constrained weighted LS (SCWLS), is additionally taken into consideration for comparison. The convex programs and systems of differential equations [21] are handled using the CVX package [41] and MATLAB ODE solver, respectively. Prior information required for the implementation of each algorithm is assumed to be perfectly input as stated in Table 1, and the algorithmic parameters of all the existing approaches remain the same as in their respective work. In particular, the values held in the neurons of Welsch-PNN

are initialized randomly from the interval $(0, 1)$ using MATLAB command `rand`. For generating the timestamps needed in invoking Welsch-PNN and SDP-TOA, we simply let the source onset time be 0.1 s and the signal propagation speed² be 1 m/s. The augmented Lagrangian parameter is set as $\rho = 5$, since we observed that this value always makes the PNN reach its equilibrium state within several tens of time constants.

Unless mentioned otherwise, we consider a deterministic deployment of sensors and source with $\mathbf{X} = \begin{bmatrix} -10 & 0 & 10 & 10 & 10 & 0 & -10 & -10 \\ 10 & 10 & 10 & 0 & -10 & -10 & -10 & 0 \end{bmatrix}$ m, $d = 2$, $L = 8$, and $\mathbf{x} = [2, 3]^T$ m. The variance of the Gaussian noise n_i , i.e., σ_i^2 , is assumed to be of identical value 0.1 m² for all i s, and the possible NLOS error q_i is randomly drawn from a uniform distribution $\mathcal{U}(0, \omega_i)$ with parameter $\omega_i \geq 0$. In tests in need of quantifying the localization accuracy, we employ the root mean square error (RMSE) with 500 ensemble Monte Carlo (MC) trials as the primary performance measure, which is calculated as $\text{RMSE} = \sqrt{\frac{1}{500} \sum_{i=1}^{500} \|\tilde{\mathbf{x}}^{\{i\}} - \mathbf{x}^{\{i\}}\|_2^2}$ with $\tilde{\mathbf{x}}^{\{i\}}$ being the estimate of source location $\mathbf{x}^{\{i\}}$ in the i th MC run. The numbers of LOS and NLOS connections are denoted by L_{LOS} and L_{NLOS} , respectively. All the numerical investigations are conducted on a computer with Intel Core i7-10710U processor and 16 GB memory.

A crucial issue in regard to the Welsch loss based robustification is how should one appropriately select the performance-decisive σ . Roughly speaking, a comparatively small σ may result in higher estimation accuracy, and the resulting criterion performs outstandingly when σ is in the range of $[0.2, 2]$ (see the early investigations in [37]). Fig. 2 plots the RMSE versus $\sigma \in [0.1, 1.9]$ in the LOS and two NLOS environments, where we have $\omega_i = 5$ and 0 for NLOS and LOS path(s), respectively. It is observed that altering σ has almost no influence on the localization performance of Welsch-PNN under LOS propagation

²This also prevents loss of precision incurred in dividing the distances by speed of light/sound.

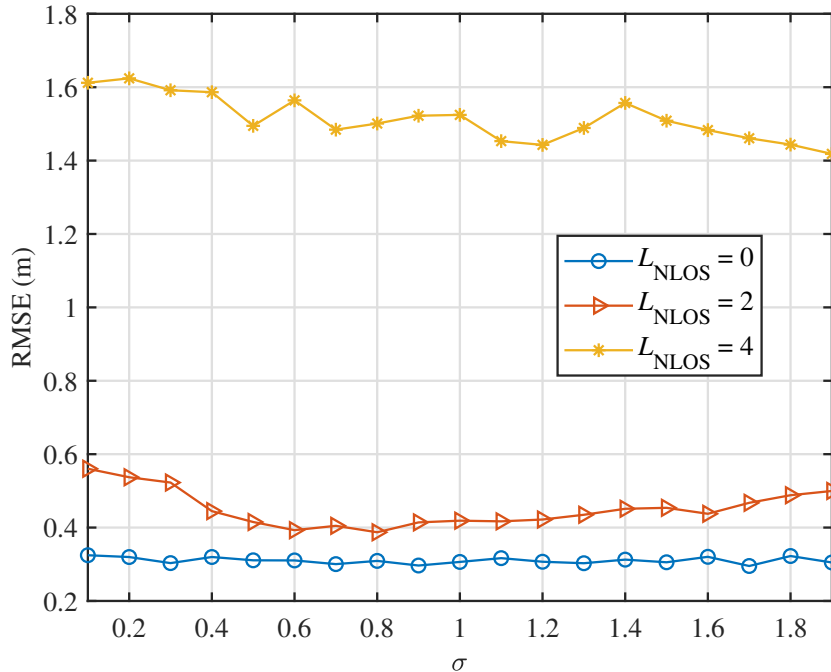


Fig. 2. RMSE versus σ in different scenarios when $L_{\text{NLOS}} = 0, 2, 4$.

while the variations in RMSE values for the NLOS scenarios are rather small (within 0.2 m) as well, offering a fair amount of flexibility. Apart from the fixed-value scheme, there exist also adaptive updating rules such as the Silverman’s heuristic [42] with σ being prudently adjusted at each iteration, which can strike a nicer balance between the efficiency and accuracy. Nevertheless, in consideration of the stability of PNN, we simply choose the parameter as $\sigma = 0.8$ throughout the whole section.

Fig. 3 plots the RMSE versus uniform distribution parameter b and empirical cumulative distribution function (CDF) of the Euclidean distance between source position and its estimate. Two NLOS scenarios are considered like those in Fig. 2. Concretely, two and four source-sensor paths are designated as NLOS ones on behalf of the mild and moderate NLOS environments, respectively, and we assign an identical value b to the parameters of uniform distribution for all

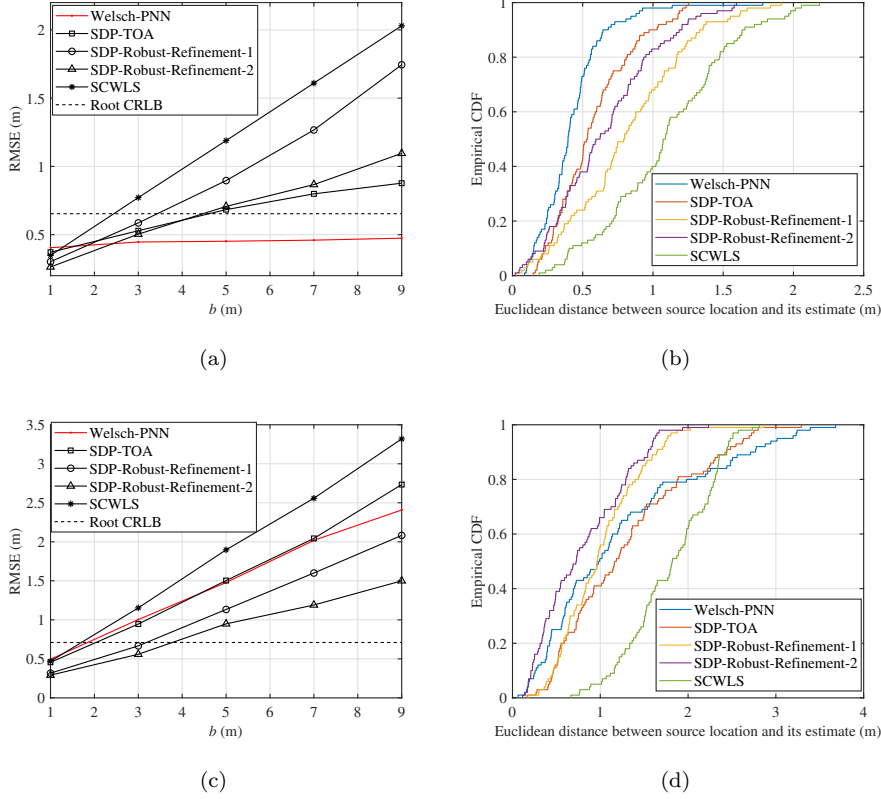


Fig. 3. RMSE and empirical CDF for considered algorithms as a function of uniform distribution parameter b and Euclidean distance between source location and its estimate in two NLOS scenarios. (a) $L_{\text{NLOS}} = 2, \omega_1 = \omega_2 = b$. (b) $L_{\text{NLOS}} = 2, \omega_1 = \omega_2 = 5$. (c) $L_{\text{NLOS}} = 4, \omega_1 = \omega_2 = \omega_3 = \omega_4 = b$. (d) $L_{\text{NLOS}} = 4, \omega_1 = \omega_2 = \omega_3 = \omega_4 = 5$.

NLOS paths. The Cramér-Rao lower bound (CRLB) when no *a priori* NLOS statistics are available [43] is also included if applicable, serving as a benchmark for performance comparison. Obviously, the non-robust SCWLS approach in general performs the worst under NLOS conditions, and the localization accuracy of all these methods degrades as b increases. Figs. 3 (a) and 3 (b) show that Welsch-PNN provides the best robustness in the mild NLOS scenario, especially when b tends to be abnormally large (viz., in the extreme NLOS environment). This is reasonable, and can be explained as the loss function we

utilize saturates and becomes like the ℓ_0 -norm³ once the fitting error exceeds a certain threshold (see [37] and Fig. 1). Moreover, we see from Fig. 3 (a) that Welsch-PNN is the only solution producing lower RMSE values than the root CRLB (using only LOS measurements) for the whole range of b . In the moderate NLOS scenario, Fig. 3 (c) illustrates that Welsch-PNN and SDP-TOA have similar performance, and are inferior to SDP-Robust-Refinement-1 and SDP-Robust-Refinement-2. Nonetheless, the former two methods benefit from much lower demand of *a priori* information and computational resources compared with the latter two, which put in extra request for the upper bounds on NLOS errors and require longer running time to solve the large-scale semidefinite programs. As showcased in Fig. 3 (d), the larger probabilities of Welsch-PNN’s Euclidean distance taking on a value ≤ 0.95 than SDP-Robust-Refinement-1’s and a value ≤ 1.9 than SDP-TOA’s also exhibit some form of performance improvement.

The discrepancy in superiority of Welsch-PNN between Figs. 3 (a) and 3 (c) motivates us to investigate the impact of sparsity of NLOS connections on the positioning accuracy. Fig. 4 plots the RMSE versus $L_{\text{LOS}} \in [4, 20]$ while fixing the number of NLOS paths as $L_{\text{NLOS}} = 4$. The parameter settings for the NLOS signals are kept the same as those in the aforementioned moderate NLOS scenario, and the positions of the newly added sensors are all randomly selected from a $20 \text{ m} \times 20 \text{ m}$ square region centered at the origin. We observe that SCWLS fails in achieving tolerable performance for all $L_{\text{LOS}}(s)$, and Welsch-PNN performs the best among all the methods for $L_{\text{LOS}} \geq 9$. In addition, Welsch-PNN attains $\text{RMSE} \leq \text{Root CRLB}$ when $L_{\text{LOS}} \geq 12$. These results further validate the superior performance of Welsch-PNN in cases where the NLOS paths tend to exhibit sparsity.

³Note that the “ ℓ_0 -norm” corresponding to the cardinality is actually not a norm, yet we call in this way by simply following the conventions.

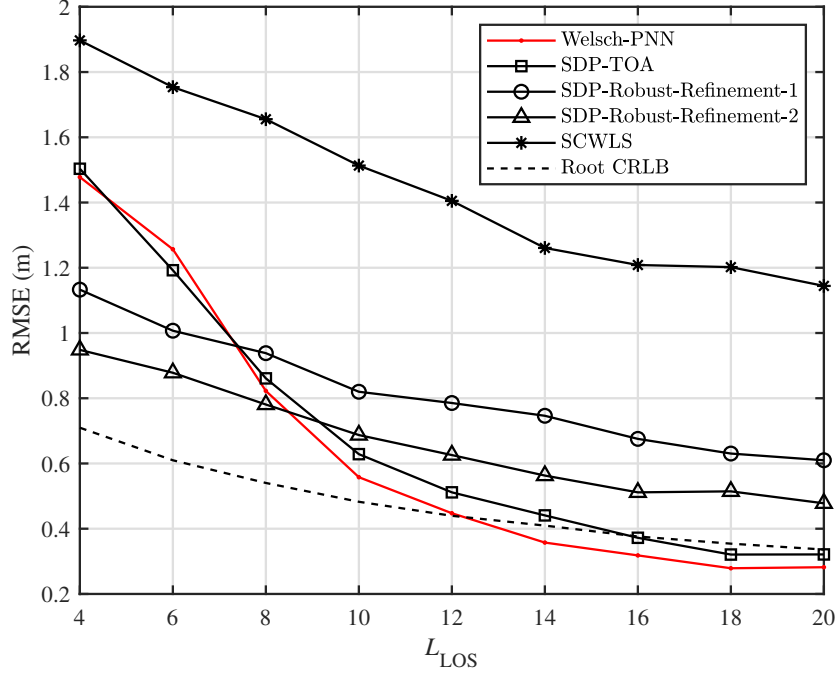


Fig. 4. RMSE versus L_{LOS} while fixing L_{NLOS} at 4.

6. Conclusion

Making use of a Welsch M -estimator based robust loss function, we have proposed an IoT applicative neurodynamic optimization scheme for TDOA localization under NLOS propagation. It has been demonstrated that our neurodynamic approach is superior to the state-of-the-art numerical methods in terms of real-time capability, localization performance, and/or prior knowledge demand.

References

- [1] K. Lin, M. Chen, J. Deng, M. M. Hassan, and G. Fortino, “Enhanced fingerprinting and trajectory prediction for IoT localization in smart build-

- ings,” *IEEE Trans. Autom. Sci. Eng.*, vol. 13, no. 3, pp. 1294–1307, Jul. 2016.
- [2] F. Khelifi, A. Bradai, A. Benslimane, P. Rawat and M. Atri, “A survey of localization systems in Internet of Things,” *Mobile Netw. Appl.*, vol. 24, no. 3, pp. 761–785, Jun. 2019.
- [3] N. Ono, H. Kohno, N. Ito, and S. Sagayama, “Blind alignment of asynchronously recorded signals for distributed microphone array,” in *Proc. IEEE Workshop Appl. Signal Process. Audio Acoustics*, New York, NY, USA, 2009, pp. 161–164.
- [4] K. C. Ho, “Bias reduction for an explicit solution of source localization using TDOA,” *IEEE Trans. Signal Process.*, vol. 60, no. 5, pp. 2101–2114, May 2012.
- [5] L. Lin, H. C. So, F. K. W. Chan, Y. T. Chan, and K. C. Ho, “A new constrained weighted least squares algorithm for TDOA-based localization,” *Signal Process.*, vol. 93, no. 11, pp. 2872–2878, 2013.
- [6] Y. Sun, K. C. Ho, and Q. Wan, “Solution and analysis of TDOA localization of a near or distant source in closed form,” *IEEE Trans. Signal Process.*, vol. 67, no. 2, pp. 320–335, Jan. 2019.
- [7] A. A. Ghany, B. Uguen and D. Lemur, “A parametric TDoA technique in the IoT localization context,” in *Proc. 16th IEEE Workshop Position., Navig., Commun. (WPNC)*, Bremen, Germany, Oct. 2019, pp. 1–6.
- [8] D. Plets, N. Podevijn, J. Trogh, L. Martens, and W. Joseph, “Experimental performance evaluation of outdoor TDoA and RSS positioning in a public LoRa network,” in *Proc. 2018 Int. Conf. Indoor Positioning Indoor Navig. (IPIN)*, Nantes, France, 2018, pp. 1–8
- [9] I. Guvenc and C.-C. Chong, “A survey on TOA based wireless localization and NLOS mitigation techniques,” *IEEE Commun. Surveys Tuts.*, vol. 11, no. 3, pp. 107–124, Aug. 2009.

- [10] C. Xu, M. Ji, Y. Qi, and X. Zhou, “MCC-CKF: A distance constrained Kalman filter method for indoor TOA localization applications,” *Electronics*, vol. 8, no. 5, p. 478, Apr. 2019.
- [11] F. Xiao, W. Liu, Z. Li, L. Chen, and R. Wang, “Noise-tolerant wireless sensor networks localization via multinorms regularized matrix completion,” *IEEE Trans. Veh. Technol.*, vol. 67, no. 3, pp. 2409–2419, Mar. 2018.
- [12] Y. Zhu, B. Deng, A. Jiang, X. Liu, Y. Tang, and X. Yao, “ADMM-based TDOA estimation,” *IEEE Commun. Lett.*, vol. 22, no. 7, pp. 1406–1409, Jul. 2018.
- [13] J. Velasco, D. Pizarro, J. Macias-Guarasa, and A. Asaei, “TDOA matrices: Algebraic properties and their application to robust denoising with missing data,” *IEEE Trans. Signal Process.*, vol. 64, no. 20, pp. 5242–5254, Oct. 2016.
- [14] M. R. Gholami, S. Gezici, and E. G. Strom, “A concave-convex procedure for TDOA based positioning,” *IEEE Commun. Lett.*, vol. 17, no. 4, pp. 765–768, Apr. 2013.
- [15] J. A. Apolinário, H. Yazdanpanah, A. S. Nascimento, and M. L. R. de Campos, “A data-selective LS solution to TDOA-based source localization,” in *Proc. IEEE Int. Conf. Acoust., Speech Signal Process. (ICASSP)*, Brighton, United Kingdom, May. 2019, pp. 4400–4404.
- [16] M. Compagnoni, A. Pini, A. Canclini, P. Bestagini, F. Antonacci, S. Tubaro, and A. Sarti, “A geometrical–statistical approach to outlier removal for TDOA measurements,” *IEEE Trans. Signal Process.*, vol. 65, no. 15, pp. 3960–3975, Aug. 2017.
- [17] G. Wang, A. M. C. So, and Y. Li, “Robust convex approximation methods for TDOA-based localization under NLOS conditions,” *IEEE Trans. Signal Process.*, vol. 64, no. 13, pp. 3281–3296, Jul. 2016.

- [18] G. Wang, W. Zhu and N. Ansari, “Robust TDOA-based localization for IoT via joint source position and NLOS error estimation,” *IEEE Internet Things J.*, vol. 6, no. 5, pp. 8529–8541, Oct. 2019.
- [19] W. Wang, G. Wang, F. Zhang, and Y. Li, “Second-order cone relaxation for TDOA-based localization under mixed LOS/NLOS conditions,” *IEEE Signal Process. Lett.*, vol. 23, no. 12, pp. 1872–1876, Dec. 2016.
- [20] Z. Su, G. Shao, and H. Liu, “Semidefinite programming for NLOS error mitigation in TDOA localization,” *IEEE Commun. Lett.*, vol. 22, no. 7, pp. 1430–1433, Jul. 2018.
- [21] W. Xiong, C. Schindelhauer, H. C. So, J. Bordoy, A. Gabbrielli, and J. Liang, “TDOA-based localization with NLOS mitigation via robust model transformation and neurodynamic optimization,” *Signal Process.*, vol. 178, 107774, Jan. 2021. Available: <https://arxiv.org/abs/2004.10492>.
- [22] R. M. Vaghefi and R. M. Buehrer, “Cooperative localization in NLOS environments using semidefinite programming,” *IEEE Commun. Lett.*, vol. 19, no. 8, pp. 1382–1385, Aug. 2015.
- [23] G. Wang, H. Chen, Y. Li, and N. Ansari, “NLOS error mitigation for TOA-based localization via convex relaxation,” *IEEE Trans. Wireless Commun.*, vol. 13, no. 8, pp. 4119–4131, Aug. 2014.
- [24] D. Tank and J. Hopfield, “Simple ‘neural’ optimization networks: An A/D converter, signal decision circuit, and a linear programming circuit,” *IEEE Trans. Circuits Syst.*, vol. 33, no. 5, pp. 533–541, May 1986.
- [25] H. Che and J. Wang, “A collaborative neurodynamic approach to global and combinatorial optimization,” *Neural Netw.*, vol. 114, pp. 15–27, Jun. 2019.
- [26] X. Hu and J. Wang, “Convergence of a recurrent neural network for non-convex optimization based on an augmented Lagrangian function,” in *Proc. 4th Int. Symp. Neural Netw.*, Nanjing, China, Jun. 2007, pp. 194–203.

- [27] M. P. Kennedy and L. O. Chua, “Neural networks for nonlinear programming,” *IEEE Trans. Circuits Syst.*, vol. 35, no. 5, pp. 554–562, May 1988.
- [28] S. Zhang and A. G. Constantinides, “Lagrange programming neural networks,” *IEEE Trans. Circuits Syst. II: Anal. Digit. Signal Process.*, vol. 39, no. 7, pp. 441–452, Jul. 1992.
- [29] Z. Yan, J. Fan, and J. Wang, “A collective neurodynamic approach to constrained global optimization,” *IEEE Trans. Neural Netw. Learn. Syst.*, vol. 28, no. 5, pp. 1206–1215, May 2017.
- [30] A. Fayyazi, M. Ansari, M. Kamal, A. Afzali-Kusha, and M. Pedram, “An ultra low-power memristive neuromorphic circuit for Internet of Things smart sensors,” *IEEE Internet Things J.*, vol. 5, no. 2, pp. 1011–1022, Apr. 2018.
- [31] Z. Han, C. S. Leung, H. C. So, and A. G. Constantinides, “Augmented Lagrange programming neural network for localization using time-difference-of-arrival measurements,” *IEEE Trans. Neural Netw. Learn. Syst.*, vol. 29, no. 8, pp. 3879–3884, Aug. 2018.
- [32] F. D. Mandanas and C. L. Kotropoulos, “Robust multidimensional scaling using a maximum correntropy criterion,” *IEEE Trans. Signal Process.*, vol. 65, no. 4, pp. 919–932, Feb. 2016.
- [33] Y. Yang, Y. Feng, and J. Suykens, “Robust low-rank tensor recovery with regularized redescending M-estimator,” *IEEE Trans. Neural Netw. Learn. Syst.*, vol. 27, no. 9, pp. 1933–1946, Sep. 2015.
- [34] C.-C. Lee, Y.-C. Chiang, C.-Y. Shih, and C.-L. Tsai, “Noisy time series prediction using M-estimator based robust radial basis function neural networks with growing and pruning techniques,” *Expert Syst. Appl.*, vol. 36, no. 3, pp. 4717–4724, 2009.

- [35] J. C. Principe, *Information Theoretic Learning: Renyi's Entropy and Kernel Perspectives*. New York, NY, USA: Springer Science & Business Media, 2010.
- [36] A. M. Zoubir, V. Koivunen, E. Ollila, and M. Muma, *Robust Statistics for Signal Processing*. Cambridge, U.K.: Cambridge Univ. Press, 2018.
- [37] W. Liu, P. P. Pokharel, and J. C. Principe, "Correntropy: Properties and applications in non-Gaussian signal processing," *IEEE Trans. Signal Process.*, vol. 55, no. 11, pp. 5286–5298, Nov. 2007.
- [38] J. Liang, C. S. Leung, and H. C. So, "Lagrange programming neural network approach for target localization in distributed MIMO radar," *IEEE Trans. Signal Process.*, vol. 64, no. 6, pp. 1574–1585, Mar. 2016.
- [39] E. Hildebrand, *Introduction to Numerical Analysis*. New York, NY, USA: Dover, 1987.
- [40] L. Lin, H. C. So, F. K. W. Chan, Y. T. Chan, and K. C. Ho, "A new constrained weighted least squares algorithm for TDOA-based localization," *Signal Process.*, vol. 93, no. 11, pp. 2872–2878, 2013.
- [41] M. Grant and S. Boyd, "CVX: MATLAB software for disciplined convex programming, version 2.1." [Online]. Available: <http://cvxr.com/cvx>
- [42] B. W. Silverman, *Density Estimation for Statistics and Data Analysis*. London, U.K.: Chapman and Hall, 1986.
- [43] Y. Qi, H. Kobayashi, and H. Suda, "Analysis of wireless geolocation in a non-line-of-sight environment," *IEEE Trans. Wireless Commun.*, vol. 5, no. 3, pp. 672–681, Mar. 2006.